Eur. Phys. J. D **12**, 509–511 (2000)

THE EUROPEAN PHYSICAL JOURNAL D

EDP Sciences

Analysis of the impedance mismatch effect in foam-solid targets compressed by laser-driven shock waves

M. Temporal[1], S. Atzeni[2], D. Batani[3], and M. Koenig[1,a]

[1] Laboratoire LULI[b], CNRS–CEA–École Polytechnique–Université Pierre et Marie Curie, 91128 Palaiseau, France
[2] Dipartimento di Energetica, Università degli Studi di Roma "La Sapienza", via A. Scarpa 14, 00161 Roma, Italy and
Associazione EURATOM-ENEA sulla Fusione, Centro Ricerche Frascati, 00044 Frascati, Italy
[3] Dipartimento di Fisica "G. Occhialini" and INFM, Università degli Studi di Milano Bicocca, via Emanueli 15, 20146 Milano, Italy

Received 20 January 2000 and Received in final form 16 May 2000

Abstract. The impedance mismatch effect in a two-layer (low density plastic foam, and solid aluminum, respectively) plane target compressed by a laser driven shock wave is considered. In such targets the ablative pressure generated by absorption of laser light in the foam layer is amplified when crossing the foam-aluminum interface. In this paper an analytical model is developed to evaluate the shock pressure in the aluminum layer as a function of the density and thickness of the foam layer and of the laser parameters. The model is in good agreement with previously published experimental results [A. Benuzzi *et al.*, Phys. Plasmas **5**, 2827 (1998)].

PACS. 52.50.Jm Plasma production and heating by laser beams – 52.50.Lp Plasma production and heating by shock waves and compression – 44.30.+v Heat flow in porous media

1 Introduction

A stationary shock wave generated in a homogeneous material is amplified when crossing the interface separating this first material from a second, denser one (see, *e.g.* Sect. XI.12 of Ref. [1]). This well known effect, resulting from the so-called impedance mismatch between the two materials, and exploited *e.g.* in experiments on equation-of-state measurement by laser driven shock waves (see [2] and references therein), has recently received renewed interest following the proposals to use very low density foam layers as outer coatings of inertial confinement fusion (ICF) solid shells [3–5], and as shock-generating layers in laser-driven shock-wave experiments [6]. In ICF, such foam layers are primarily used for mitigating laser non-uniformities, but pressure amplification is also of interest, as a positive side-effect. In shock wave experiments foam layers are introduced just as pressure "amplifiers".

Recently, pressure amplification due to impedance-mismatch has been addressed by an experiment [7] performed at the Laboratoire pour l'Utilisation des Laser Intenses. A pulsed laser beam (with energy $E_{\rm L} \leq 100$ J, wavelength $\lambda = 0.53$ μm, and Gaussian shape in time, with full width at half maximum of 600 ps) was focused with peak intensity intensity $I = (2{-}5) \times 10^{13}$ W/cm^2 onto a target (see Fig. 1) made of a plastic foam layer [8] (with thickness $\Delta_{\rm f} = 50$ μm, and density in the range $5 < \rho_{\rm f} < 1000$ mg/cm^3), supported by an aluminum base (with density $\rho_{\rm Al} = 2.7$ g/cm^3). Rear-side imaging, coupled to a visible streak camera, provided the measurement of the shock transit time Δt through the aluminum steps at the rear side of the target, thus allowing for the evaluation of the shock velocity $D_{\rm Al}$. The shock pressure $P_{\rm Al}$ was then computed by using the Hugoniot relations and the equation-of-state data provided by the SESAME tables [9].

The experimental data [7] show that, starting from relatively large foam density, the pressure $P_{\rm Al}$ measured in the aluminum layer, at first increases as the foam density $\rho_{\rm f}$ decreases, but for $\rho_{\rm f}$ below a certain characteristic density $\rho_{\rm c}$, $P_{\rm Al}$ decreases. Such a behavior seems to disagree with the expected pressure amplification by impedance mismatch. In fact, we show in this paper that a simple analytical model explains the experimental data, and the pressure amplification by impedance mismatch is always increasing with the density ratio $\rho_{\rm Al}/\rho_{\rm f}$. The decrease of the measured pressure at the lowest foam densities only follows from the fact that, for this particular experimental set-up, at the lowest foam densities the shock reaches the interface when the laser pulse has not yet reached its peak value. The reduced pressure in the aluminum is therefore resulting from the lower pressure of the primary shock, and not by a reduced shock amplification at the interface.

[a] e-mail: koenig@greco2.polytechnique.fr
[b] Unité Mixte n° 7605

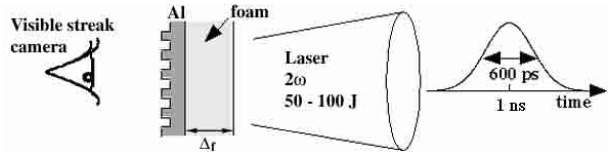

Fig. 1. Scheme of the target and laser parameters.

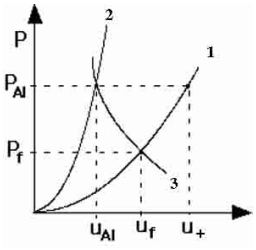

Fig. 2. Shock characteristics in the u-P plane. 1: Shock polar in foam, 2: shock polar in Al, 3: transmitted shock in Al.

2 Analytical model

The model is based on the standard theory (*e.g.* Chap. I of Ref. [1]) of strong, steady, one-dimensional plane shocks of pressure P propagating through a material with initial density ρ and initial pressure $P_0 \ll P$. It is further assumed that, as far as shock propagation is concerned, materials can be described by a perfect gas ideal equation of state, according to which pressure P, mass density ρ and specific energy ε are related by $P = (\gamma - 1)\rho\varepsilon$. We shall assume adiabatic index $\gamma = 5/3$ for all materials, but generalization to any value γ is straightforward. Within such a model, the velocity D of the shock wave, and the velocity u of the shocked fluid behind the shock wave are related to the shock pressure P and to the density ρ of the uncompressed material by $u^2 = [2/(\gamma+1)]P/\rho$, and $D^2 = [(\gamma+1)/2]P/\rho$. We also assume that the transmitted shock at the foam-Al interface can be represented, on the u-P plane, by the specular curve of the incoming shock in the foam (Fig. 2). This last assumption is standard and accurate for weak shock waves (see Sect. XI.12 of Ref. [1]), but numerical simulations we performed with the fluid-dynamics code DUED [10] indicate that it is still acceptable in the present case.

We now consider the fluid velocities u_f and u_Al associated with the shock pressures P_f and P_Al reached in the foam layer and in the aluminum layer, respectively. We also call u_+ the fluid velocity that would be achieved in the foam layer if it were subjected to a shock of pressure P_Al (see Fig. 2). It is apparent that we can write $u_\mathrm{Al} = u_\mathrm{f} - (u_+ - u_\mathrm{f}) = 2u_\mathrm{f} - u_+$ with

$$u_\mathrm{f} = \left[\frac{2P_\mathrm{f}}{(\gamma+1)\rho_\mathrm{f}}\right]^{1/2}; \quad u_+ = \left[\frac{2P_\mathrm{Al}}{(\gamma+1)\rho_\mathrm{f}}\right]^{1/2}. \tag{1}$$

From the conservation equations at the shock front we have:

$$P_\mathrm{Al} = \left[\frac{2}{(\gamma+1)}\right]\rho_\mathrm{Al}D_\mathrm{Al}^2; \tag{2}$$

$$D_\mathrm{Al} = \frac{(\gamma+1)}{2}u_\mathrm{Al} = \frac{(\gamma+1)}{2}\left\{2\left[\frac{2P_\mathrm{f}}{(\gamma+1)\rho_\mathrm{f}}\right]^{1/2} - \left[\frac{2P_\mathrm{Al}}{(\gamma+1)\rho_\mathrm{f}}\right]^{1/2}\right\}. \tag{3a}$$

Substituting equation (2) for P_Al into equation (3a), and solving for D_Al, we get the shock velocity in the denser layer (aluminum) as a function of the pressure P_f of the shock in the foam layer and of the densities of the two layers

$$D_\mathrm{Al} = \frac{[2(\gamma+1)]^{1/2}}{\rho_\mathrm{f}^{1/2} + \rho_\mathrm{Al}^{1/2}}P_\mathrm{f}^{1/2}. \tag{3b}$$

The pressure of the shock in the aluminum layer is then found by substituting equation (3b) into equation (2), thus getting

$$P_\mathrm{Al} = \frac{4}{\left[1 + (\rho_\mathrm{f}/\rho_\mathrm{Al})^{1/2}\right]^2}P_\mathrm{f}. \tag{4}$$

Equations (3b, 4) represent the impedance-mismatch effect: for a given primary shock pressure P_f, the velocity D_Al of the shock launched into the denser aluminum layer increases as the density of the first layer decreases.

In the experiment the shock wave is generated by the laser driven ablative pressure. A good approximation to the ablative pressure generated in a plastic material by a laser pulse of constant intensity I, and wavelength λ, focussed onto a spot of radius r_L is given by

$$P[\mathrm{Mbar}] = 12[I/(10^{14}\ \mathrm{W/cm^2})]^{7/9} \times [r_\mathrm{L}/100\ \mu\mathrm{m})]^{-1/9}[\lambda(\mu\mathrm{m})]^{-2/9}. \tag{5}$$

(such a scaling was first proposed in Ref. [11], the front factor was given in Ref. [12], and a comparison with experiments and simulation can be found in Ref. [13]).

The actual laser pulse is however shaped in time. Extensive numerical simulations performed with the radiation-hydrodynamics code DUED [10] indicate that in the whole range of parameters of the experiment of reference [7] a good approximation to the speed of the shock front in the foam layer is

$$D(t) = \begin{cases} D_\mathrm{max}\dfrac{t}{t_*} & t < t_* \\ D_\mathrm{max} & t \geq t_* \end{cases} \tag{6}$$

where $D_\mathrm{max} = [(\gamma+1)P_*/2\rho_\mathrm{f}]^{1/2}$ is the value of the shock velocity corresponding to a constant pressure equal to the value of the ablative pressure P_* computed by using equation (5) with the peak laser intensity I, and t_* is a characteristic time, close to the time at which laser intensity reaches its maximum value. Simulations also show that effects due to radiative transfer do not affect propagation of shocks in the present experiment.

From equation (6) it follows that, for $t < t_*$ the velocity of the shock front at depth y in the foam layer is $D_\mathrm{f}(y) = (2yD_\mathrm{max}/t_*)^{1/2}$. Therefore the shock velocity and pressure when the foam-aluminum interface ($y = \Delta_\mathrm{f}$) is reached, are respectively,

$$D_\mathrm{f} = D(\Delta_\mathrm{f}) = \begin{cases} \left(\dfrac{2\Delta_\mathrm{f}D_\mathrm{max}}{t_*}\right)^{1/2} & t(\Delta_\mathrm{f}) < t_* \\ D_\mathrm{max} & t(\Delta_\mathrm{f}) \geq t_* \end{cases} \tag{7}$$

and

$$P_{\rm f} = \begin{cases} \dfrac{2\Delta_{\rm f}}{t_*}\left(\dfrac{2P_*}{\rho(\gamma+1)}\right)^{1/2} & t(\Delta_{\rm f}) < t_* \\ P_* & t(\Delta_{\rm f}) \geq t_* \end{cases}. \quad (8)$$

Notice that the condition $t(\Delta_{\rm f}) < t_*$ can also be written $\Delta_{\rm f} < D_{\max} t_*/2$, or

$$\rho_{\rm f} < \rho_{\rm c} = \frac{(\gamma+1)t_*^2 P_*}{8\Delta_{\rm f}^2}, \quad (9)$$

showing the existence of a *characteristic foam density*, $\rho_{\rm c}$, which discriminates between the two cases.

By using equation (3b) we can finally write the shock velocity $D_{\rm Al}$ and the pressure $P_{\rm Al}$ into the aluminum as:

$$D_{\rm Al} = \begin{cases} \dfrac{[2(\gamma+1)]^{1/2}}{\rho_{\rm f}^{1/2}+\rho_{\rm Al}^{1/2}} P_*^{1/2} & \rho_{\rm f} \geq \rho_{\rm c} \quad (10a) \\ \dfrac{2(\gamma+1)^{1/4}(2\rho_{\rm f}P_*)^{1/4}}{\left(\rho_{\rm f}^{1/2}+\rho_{\rm Al}^{1/2}\right)}\left(\dfrac{\Delta_{\rm f}}{t_*}\right)^{1/2} & \rho_{\rm f} < \rho_{\rm c} \quad (10b) \end{cases}$$

and

$$P_{\rm Al} = \begin{cases} \dfrac{4}{\left(1+(\rho_{\rm f}/\rho_{\rm Al})^{1/2}\right)^2} P_* & \rho_{\rm f} \geq \rho_{\rm c} \quad (11a) \\ \dfrac{8(2P_*)^{1/2}}{(\gamma+1)^{1/2}\left[1+(\rho_{\rm f}/\rho_{\rm Al})^{1/2}\right]^2}\dfrac{\rho_{\rm f}\Delta_{\rm f}}{\rho_{\rm f}^{1/2}t_*} & \rho_{\rm f} < \rho_{\rm c}. \quad (11b) \end{cases}$$

Equation (11b) shows that for family of targets with $\rho_{\rm f} < \rho_{\rm c}$ and fixed value of $\rho_{\rm f}\Delta_{\rm f}$, the pressure $P_{\rm Al}$ increases as the foam density decreases (and for $\rho_{\rm f} \ll \rho_{\rm Al}$, one has $P_{\rm Al} \propto \rho_{\rm f}^{-1/2}$); for families of targets with given thickness of the foam layer $\Delta_{\rm f}$, instead, the pressure $P_{\rm Al}$ increases with the foam density.

We now apply the model to the quoted LULI experimental parameters [7], namely, $\Delta_{\rm f} = 50$ μm, $\lambda = 0.53$ μm, $r_{\rm L} = 100$ μm, and two different values of the laser intensity, $I \cong 5 \times 10^{13}$ W/cm^2, and $I \cong 2 \times 10^{13}$ W/cm^2. We also take $t_* = 800$ ps (the laser intensity reaching its maximum about $t = 1$ ns). Model results for the pressure measured in the aluminum layer *versus* the foam density are presented in Figure 3 (solid curves), together with experimental data. A satisfactory agreement is found. The values of the characteristic critical density obtained from equation (9), ($\rho_{\rm c} = 34$ mg/cm^3 and 68 mg/cm^3, respectively) are also seen to approximately agree with the experimental data.

3 Conclusions

We have presented a simple analytical model for the interpretation of a set of experimental data concerning pressure measurements in two-layer (plastic foam and aluminum) targets compressed by shock waves ablatively generated by laser absorption in the foam layer. The model reproduces the behavior of the pressure detected experimentally. It is apparent that the measured pressure results from the pressure of the laser driven shock wave in the foam, amplified by the density mismatch at the interface. For certain target parameters the reduced pressure measured at the lowest foam density does not depend on some unexpected modifications of the impedance-mismatch effect, but just on the lower pressure of the shock reaching the interface. Indeed, in such cases the foam layer areal mass is so small that the laser driven shock reaches the interface well before the laser pulse reaches peak intensity. We established that a characteristic critical foam density $\rho_{\rm c}$ (which depends on a characteristic time related to the laser pulse rise time and on the thickness of the foam layer, see Eq. (9)) discriminates two regimes: for density $\rho_{\rm f} > \rho_{\rm c}$ the pressure in the aluminum layer increases as the foam density decreases; for $\rho_{\rm f} < \rho_{\rm c}$, the behavior is reversed.

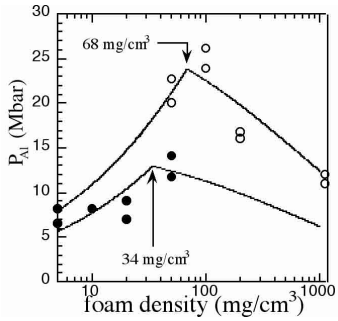

Fig. 3. Aluminum pressure *versus* foam density. Solid curves: analytical results; circles: experimental results. Upper curve and void circles refer to $I = 5 \times 10^{13}$ W/cm^2; lower curve and filled circles to $I = 2 \times 10^{13}$ W/cm^2.

This work was supported by the E.U. TMR program under contract ERBFMGE-CT95-0044.

References

1. Y.B. Zeldovich, Y.P. Raizer, *Physics of shock waves and high temperature hydrodynamic phenomena* (Academic Press, New York, 1967).
2. M. Koenig *et al.*, Phys. Rev. Lett. **74**, 2260 (1995).
3. M.H. Emery *et al.*, Phys. Fluids B **3**, 2640 (1991).
4. M. Desselberger *et al.*, Phys. Rev. Lett. **74**, 2961 (1995).
5. M. Dunne *et al.*, Phys. Rev. Lett. **75**, 3858 (1995).
6. N. Holmes *et al.*, Rev. Sci. Instrum. **62**, 199 (1991).
7. A. Benuzzi *et al.*, Phys. Plasmas **5**, 1827 (1998).
8. J.W. Falconer, W. Nazarov, J. Vac. Sci. Technol. A **13**, 1941 (1995).
9. SESAME: *The LANL Equation of State database*, report LA-UR-92-3407, Los Alamos National Laboratory (1992)
10. S. Atzeni, Comput. Phys. Commun. **43**, 107 (1986); the radiation multigroup diffusion scheme is summarily described in Section 11.2.5 of Nuclear Fusion Division 1994-95 Progress Report (ENEA, Roma, 1996); opacities are provided by the SNOP code by K. Eidmann, Laser Particle Beams **12**, 223 (1994).
11. A. Caruso, R. Gratton, Plasma Phys. **10**, 867 (1968).
12. P. Mora, Phys. Fluids **25**, 1051 (1982).
13. S. Atzeni, Plasma Phys. Control. Fusion **29**, 1535 (1987).